DOI: 10.1534/genetics.104.033647

The Meiotic Recombination Hot Spot *ura4A* in *Schizosaccharomyces pombe*

Michel Baur,[1] Edgar Hartsuiker,[2] Elisabeth Lehmann, Katja Ludin, Peter Munz and Juerg Kohli[3]

Institute of Cell Biology, University of Bern, CH-3012 Bern, Switzerland

Manuscript received July 16, 2004
Accepted for publication October 18, 2004

ABSTRACT

The meiotic recombination hot spot *ura4A* (formerly *ura4-aim*) of *Schizosaccharomyces pombe* was observed at the insertion of the *ura4*$^+$ gene 15 kb centromere-proximal to *ade6* on chromosome III. Crosses heterozygous for the insertion showed frequent conversion at the heterology with preferential loss of the insertion. This report concerns the characterization of 12 spontaneous *ura4A* mutants. A gradient of conversion ranging from 18% at the 5′ end to 6% at the 3′ end was detected. A novel phenomenon also was discovered: a mating-type-related bias of conversion. The allele entering with the *h*$^+$ parent acts preferentially as the acceptor for conversion (ratio of 3:2). Tetrad analysis of two-factor crosses showed that heteroduplex DNA is predominantly asymmetrical, enters from the 5′ end, and more often than not covers the entire gene. Restoration repair of markers at the 5′ end was inferred. Random spore analyses of two-factor crosses and normalization of prototroph-recombinant frequencies to physical distance led to the demonstration of map expansion: Crosses involving distant markers yielded recombinant frequencies higher than the sum of the frequencies measured in the subintervals. Finally, marker effects on recombination were defined for two of the *ura4A* mutations.

HOMOLOGOUS recombination contributes to the generation of genetic diversity and is required for proper chromosome segregation in meiosis and for the repair of DNA damage. Since homologous recombination occurs most frequently during meiosis, the underlying mechanisms are best studied in ascomycetous fungi in which all four products of single meioses can be individually recovered and analyzed (Paques and Haber 1999). The fate of the four chromatids in a diploid cell undergoing meiosis can be followed by tetrad analysis. Examination of the segregation of genetic markers in tetrads has demonstrated two classes of recombination events: the classical reciprocal exchange of DNA sequences, called crossing over, and the unidirectional transfer of genetic information between chromatids, designated non-Mendelian segregation (NMS). Two types of NMS events are distinguished. One is the nonreciprocal transfer of information of both DNA strands of a donor chromatid to a chromatid of the homologous chromosome. This segregation type is called gene conversion and manifests itself in 6+:2− or 2+:6− segregation of genetic markers. The numbers refer to the eight single strands of the tetrad with + indicating wild type and − indicating mutant information. The other unidirectional transfer changes only one strand of the recipient chromatid. The resulting spore bears both wild-type and mutant information. Since the genetic marker segregates only in the first mitotic division after meiosis, the observed 5+:3− or 3+:5− tetrads are called postmeiotic segregations (PMS).

The frequency of homologous recombination varies widely from interval to interval along the genome. DNA regions with lower or higher than average frequency of aberrant segregation and crossing over are called cold spots or hot spots, respectively. They have been identified and described in many different organisms (Lichten and Goldman 1995; Paques and Haber 1999; Petes 2001). Specific nucleotide sequences have been identified in some cases, which are recognized by proteins promoting, directly or indirectly, a rate-limiting step of the recombination process (Smith 2001).

A phenomenon often seen in intragenic studies is polarity of NMS. The frequency of NMS events falls steadily from one end of the gene to the other, indicating a preferential initiation or termination point for homologous recombination (Nicolas and Petes 1994). In the budding yeast *Saccharomyces cerevisiae*, hot spots and high NMS ends have been correlated with the occurrence of double-strand breaks (DSB) at nuclease hypersensitive sites in chromatin (Ohta *et al.* 1994; Wu and Lichten 1994; de Massy *et al.* 1995; Liu *et al.* 1995). Double-strand breaks initiating meiotic recombination have also been demonstrated in *Schizosaccharomyces pombe* (Cervantes *et al.* 2000; Steiner *et al.* 2002; Young *et al.* 2002).

[1]*Present address:* ZLB Behring AG, CH-3000 Bern 22, Switzerland.

[2]*Present address:* Genome Damage and Stability Centre, University of Sussex, Brighton BN1 9RQ, United Kingdom.

[3]*Corresponding author:* Institute of Cell Biology, University of Bern, Baltzerstr 4, CH-3012 Bern, Switzerland.
E-mail: juerg.kohli@izb.unibe.ch

For the characterization of the meiotic hot spot mutation *ade6-M26* (Gutz 1971), the flanking marker *ura4-aim*, in this article renamed *ura4A*, was constructed between *ade6* and the centromere of chromosome III. The insertion 15 kb upstream of *ade6* contains the functional *S. pombe ura4*$^+$ gene on a 1.8-kb DNA fragment (Grimm *et al.* 1994). The insertion heterology turned out to be a hot spot itself with 3.7% NMS frequency and disparity of conversion loss being 3.5 times more frequent than transfer of the insertion (Zahn-Zabal *et al.* 1995). When the *M26* hot spot is active, NMS frequency at *ura4A* is reduced, indicating competition for recombination factors by the two hot spots. The hot spot property of *ura4A* near *ade6* is possibly due to a new chromosomal context, since *ura4*$^+$ at its original locus on the left arm of chromosome III shows no elevated NMS frequency when crossed with a strain carrying the *ura4-D18* deletion (Zahn-Zabal *et al.* 1995).

To see whether *ura4A* also behaves as a hot spot in homozygous configuration, we isolated and characterized 12 spontaneous mutations within *ura4A*, tested them with respect to NMS by tetrad analysis, and determined prototroph frequencies in two-factor crosses. The highest frequencies of conversion (18%) so far recorded in fission yeast were observed. In addition, we document a novel phenomenon: a mating-type-related bias of NMS (mat bias) at *ura4A* and confirm the existence of map expansion, a phenomenon first described in classical fine-structure mapping of genes.

MATERIALS AND METHODS

Strains, media, and general genetic methods: The construction of the *ura4A*$^+$ strains GC151a and GC151b was described by Grimm *et al.* (1994). The spontaneous *ura4A*$^-$ mutants were derived from GC151a (alleles 1–6) and from GC151b (alleles 9–14; Table 1) by selection of uracil-dependent cells on minimal medium containing uracil and 5-fluoroorotic acid as described by Grimm *et al.* (1988). The isolated ura$^-$ clones were classified as *ura4A* or *ura5* using the criss-cross technique described by Gutz *et al.* (1974). *ura5* mutants were not considered further. The *ura4A* isolates are independent of each other because different starting clones were used. In the two instances in which small clusters of homoalleles were found, only one representative was kept. Standard minimal medium (MMA) consists of 0.67% Difco yeast nitrogen base without amino acids, 1% glucose, and 1.8% agar. The other standard media, yeast extract agar (YEA), malt extract agar (MEA), and the general genetic methods, are described by Gutz *et al.* (1974). Supplements were added to the media at concentrations of 0.01% (w/v).

Sequencing the *ura4A* junctions: The construction of the *ura4A* insertion has been published (Grimm *et al.* 1994). Polymerase chain reaction (PCR) fragments were generated from the genomic DNA of strain GC151b with primers KL1 (5′-gtaatgaagccagccagtcg-3′) and KL4 (5′-catgctcctacaacattaccac-3′) to give the 3′-junction fragment and KL2 (5′-tgggtacccttc caatagtctc-3′) and KL3 (5′-cacaaagtgcaaacattatcatg-3′) to result in the 5′-junction fragment. The DNA was purified using NucleoSpin Extract columns (Macherey-Nagel, Duren, Germany). The 3′-junction fragment was sequenced with KL5 (5′-tggttataaacattggtgttggaac-3′) and the 5′-junction fragment with KL6 (5′-caccatgccaaaaattacacaag-3′), respectively.

Sequencing of *ura4A* mutations: Total genomic DNA was isolated from haploid *ura4A* mutant strains (Table 1) by the small-scale method of Wright *et al.* (1986). To amplify a 1015-bp *ura4A*-specific genomic DNA fragment by PCR, two synthetic oligonucleotide primers with artificial 5′ restriction sites were designed (*Bam*HI, 5′-gcgcgVgATCCCAGTTTAACTATGCTT CGTCGGC-3′; *Eco*RI, 5′-gccggVAATTCTAAATGCCTTCTG ACATAAAACGCC-3′). The desired PCR fragment, containing the entire 792-bp *ura4* open reading frame (ORF) and including 118-bp upstream and 105-bp downstream regulatory sequences, was amplified in a 100-μl reaction volume containing 750 ng of genomic DNA, 0.25 μM of each primer, 200 μM of each dNTP, 0.5 units Super *Taq* polymerase (Stehelin, Basel Switzerland), 10 mM Tris·HCl, pH 9.0, 50 mM KCl, 1.5 mM $MgCl_2$, 0.1% Triton X-100, and 0.01% (w/v) gelatin. Reactions were performed in a Perkin-Elmer (Norwalk, CT) Cetus DNA thermal cycler as follows: 4 min at 94°, 30 cycles at 94°, 59°, and 72° for 1 min each, and 10-min extension at 72°. Phenol-extracted PCR fragments were ligated after appropriate restriction digestion into the *Bam*HI and *Eco*RI sites of pUC18 and analyzed by DNA sequencing. In addition to the two PCR primers, four internal primers had to be synthesized for the entire sequencing of both DNA strands by the dideoxy chain termination method [United States Biochemical (Cleveland) Sequenase kit]. To exclude artifacts, especially to distinguish *Taq* polymerase errors from the original *ura4A* mutations, at least three independent PCR products of each mutant were analyzed. In this way, all of the mutations in question could be located within the *ura4A* ORF.

Tetrad and octad analysis: Tetrads were dissected on YEA plates using the Singer Instruments MSM system. After 4–5 days at 30°, the grown colonies were treated further. In monofactorial crosses their constitution with respect to mating type and *ura4A* was established. The latter was done by replica plating onto medium without uracil. In this way conversion, but not PMS, can be detected because a print consisting of approximately half ura$^+$ and half ura$^-$ cells will be scored as ura$^+$.

In the heteroallelic cross X1119 = S82 × S89 = h^- *ura4A-10 ura4-D18* × h^+ *ura4A-13 ura4-D18*, the four colonies of each tetrad were streaked onto a YEA master plate and after growth were replicated on three MEA plates. The first was cross-stamped with the wild-type testers 972 (h^-) and 975 (h^+), the second with the tester pair S88/S89 (allele *13*), and the third with the pair S82/S83 (allele *10*). After this second round of mating and sporulation, the first plate was exposed to iodine vapors to determine mating type. The two others were replicated onto medium lacking uracil. Ensuing growth at the crossing between segregant and tester reflects wild-type sequence in the segregant with respect to the mutation carried by the tester. Correspondingly, no growth means that there is a mutant sequence in the segregant. In this way the allelic constitution of spores at the *ura4A* locus could be assessed: + +, + *10*, *13*+, and *13 10*. Again, single-site PMS cannot be detected in this way. On the other hand, co-PMS spores (*13*+/+*10*) are detected. Such streaks do not yield confluent growth on medium without uracil, in contrast to prototrophic recombinants. They show growth with both testers in the limited crossing areas. This interpretation was verified by plating single cells from the original streak and typing the resulting colonies: None were prototrophic; approximately half were of one parental genotype (*13*+) and half of the other type (+*10*).

An octad analysis of cross MX1124 was done. MX1124 = MU137 × MU136 = h^- *ura4A-10 ura4-D18* × h^+ *ura4A-13*

TABLE 1

***S. pombe* strains used in this study**

Designations[a]	Genotype[b]
GC151a BSC 46-1811	h^- *ura4A*$^+$ *ura4-D18*
GC151b BSC 46-1812	h^+ *ura4A*$^+$ *ura4-D18*
S64 BSC 45-1764	h^- *ura4A-1 ura4-D18*
S65 BSC 45-1765	h^+ *ura4A-1 ura4-D18*
S66 BSC 45-1766	h^- *ura4A-2 ura4-D18*
S67 BSC 45-1767	h^+ *ura4A-2 ura4-D18*
S68 BSC 45-1768	h^- *ura4A-3 ura4-D18*
S69 BSC 45-1769	h^+ *ura4A-3 ura4-D18*
S70 BSC 45-1770	h^- *ura4A-4 ura4-D18*
S71 BSC 45-1771	h^+ *ura4A-4 ura4-D18*
S72 BSC 45-1772	h^- *ura4A-5 ura4-D18*
S73 BSC 45-1773	h^+ *ura4A-5 ura4-D18*
S74 BSC 45-1774	h^- *ura4A-6 ura4-D18*
S75 BSC 45-1775	h^+ *ura4A-6 ura4-D18*
S80 BSC 45-1780	h^- *ura4A-9 ura4-D18*
S81 BSC 45-1781	h^+ *ura4A-9 ura4-D18*
S82 BSC 45-1782	h^- *ura4A-10 ura4-D18*
S83 BSC 45-1783	h^+ *ura4A-10 ura4-D18*
S84 BSC 45-1784	h^- *ura4A-11 ura4-D18*
S85 BSC 45-1785	h^+ *ura4A-11 ura4-D18*
S86 BSC 45-1786	h^- *ura4A-12 ura4-D18*
S87 BSC 45-1787	h^+ *ura4A-12 ura4-D18*
S88 BSC 45-1788	h^- *ura4A-13 ura4-D18*
S89 BSC 45-1789	h^+ *ura4A-13 ura4-D18*
S90 BSC 45-1790	h^- *ura4A-14 ura4-D18*
S91 BSC 45-1791	h^+ *ura4A-14 ura4-D18*
OL497 BSC 84-3346	h^- *ura4A*$^+$ *ura4-D18 his3-D1 swi10::kanMX ade6-M210*
MAB039 BSC 58-2295	h^- *ura4A*$^+$ *ura4-D18 pms1::his3*$^+$ *his3-D1 ade6-M210*
MU132 BSC 97-3873	h^+ *ura4A-13 ura4-D18 his3-D1 swi10::kanMX*
MU134 BSC 97-3875	h^+ *ura4A-10 ura4-D18 his3-D1 swi10::kanMX*
MU137 BSC 98-3891	h^- *ura4A-10 ura4-D18 his3-D1 pms1::his3*$^+$ *swi10::kanMX*
MU136 BSC 98-3890	h^+ *ura4A-13 ura4-D18 his3-D1 pms1::his3*$^+$ *swi10::kanMX*

[a] The first entry is either the original strain name or a short version of the BSC number. The second entry is the number of the Berne strain collection.

[b] All strains are from this study except GC151a and GC151b (Grimm *et al.* 1994) and OL497 obtained from O. Fleck. MU132 is a segregant from cross OL497 × S89, MU134 was obtained from OL497 × S83, MU136 from MAB039 × MU132, and MU137 from MAB039 × MU134.

ura4-D18, as in X1119, but here, in contrast to X1119, both parents had inactivated repair genes, *pms1::his3*$^+$ and *swi10::kanMX*. The cross was set up in the usual way on MEA. Tetrads were dissected on YEA in the afternoon and kept 3 hr at 30°. Then plates were transferred to 18°. The next day many spores appeared pear shaped, indicating germination. Plates were placed at 30° and observed at regular intervals. If a spore produced two daughters, they were separated by micromanipulation. In the best case, upon incubation eight colonies, organized in four pairs, resulted. Since in MX1124 the same *ura4A* alleles were involved (*13* and *10*) as were involved in X1119, the same procedures and tester strains as were used to analyze spore clones in X1119 could be used to type the postmeiotic segregants.

Random spore analysis: The frequency of prototrophic recombinants was determined in heteroallelic crosses between mutants listed in Table 1. Cell material of both parental strains was suspended, mixed, and plated in a dense lawn on MEA. Incubation was 3 days at 25°. To kill vegetative cells, the sporulated material was treated over night at 30° with an aqueous snail enzyme solution [1:1000 (v/v) *Helix pomatia* juice, Biosepra]. For titer estimation of prototrophic recombinants and total spores, samples of appropriately diluted spore suspensions were spread on MMA and MMA + uracil, respectively. Incubation was 5 days at 30°.

RESULTS

Insertion junctions and *ura4A* mutants: To verify correct insertion of the *ura4A* gene according to the published procedure (Grimm *et al.* 1994), PCR fragments of the *ura4A* junctions were generated and sequenced as described in materials and methods. It was found that the *ura4A* gene is transcribed in the opposite direction to the *ade6* gene (Figure 1). While the 5′-junction (AAGCT-ATC) was exactly as predicted from the construction, the 3′-junction was found to contain an additional 15 bp of unknown origin: GAT-cctggtatggcttgt-

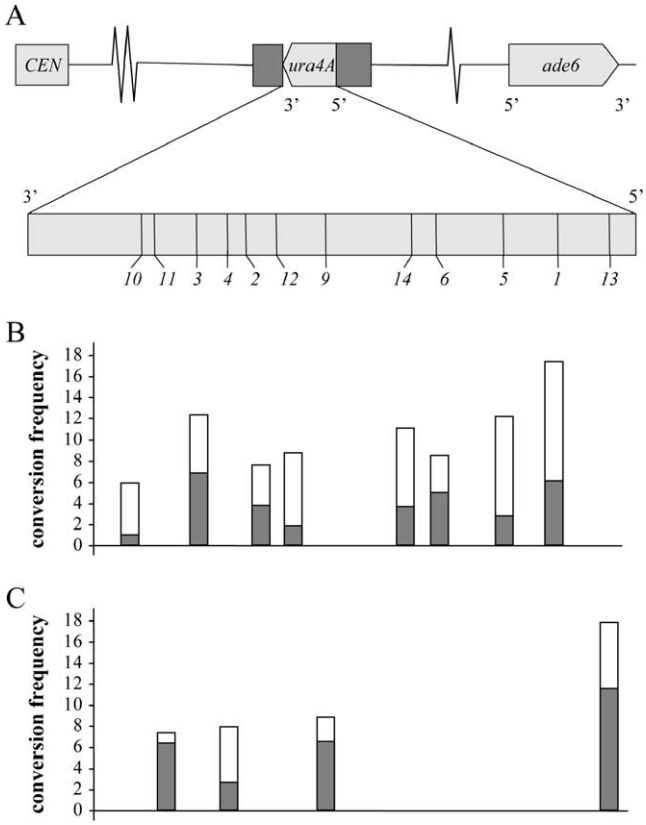

FIGURE 1.—The *ura4A* hot spot. (A, top) The location and orientation of the *ura4A* insertion on chromosome III. (A, bottom) The locations of the sequenced mutations in the open reading frame (see Table 2 for details). In B and C, a gradient of conversion frequencies (percentage of NMS of tetrads examined) is apparent with the high frequencies for the mutations at the 5′ end. (B) Tetrad analysis of type I crosses (h^+ *ura4A*$^+$ × h^- *ura4A*$^-$) yielded overall more 2:6 (open bars) than 6:2 conversions (shaded bars). (C) Type II crosses (h^- *ura4A*$^+$ × h^+ *ura4A*$^-$) yielded more 6:2 than 2:6 conversions. For further explanations see the text.

AGCTT. No full match of the 15 bp to *S. pombe* or *Escherichia coli* genomic DNA could be detected.

The *ura4A-x* mutations are of spontaneous origin. Their positions in the gene and the physical alterations are given in Table 2 and Figure 1. Most are single-base-pair changes. *ura4A-6* is a G-to-C transversion, which is known to show strongly enhanced prototroph frequencies in intragenic two-factor crosses (SCHÄR and KOHLI 1993). This is also true for this mutation (data not shown). Yet conversion frequency of *ura4A-6* in single-point crosses is comparable to the frequencies obtained with neighboring markers. *ura4A-11* is mitotically highly unstable (data not shown). This is understandable, considering its molecular nature (22-bp repeat). It cannot be used in random spore analysis of intragenic two-factor crosses. No problems arise with tetrads because the numerous matings between revertant and wild-type cells give 8+:0− segregations, which are recognized and excluded. *ura4A-11* yields a conversion frequency similar to the mutations to its left and right.

Hot spot, polarity, and mat bias as revealed by tetrad analysis: The data on tetrad analyses of monofactorial crosses are given in Table 2 and Figure 1. The overall conversion frequencies of the extreme markers to the 5′ and 3′ sides are 18% (*ura4A-13*) and 6% (*ura4A-10*). Values of intervening mutations are in between these two values. In *S. pombe* 17 multifactorial crosses producing a total of 12,119 segregations of allelic differences showed only 17 3:1 and 15 1:3 conversion tetrads, giving an average NMS frequency of 0.26% (P. MUNZ, unpublished results). The 20- to 60-fold higher conversion frequencies of the tested alleles clearly show that *ura4A* is a hot spot of meiotic recombination.

Figure 1 shows that conversion frequencies gradually decline from the 5′ to the 3′ side of the gene. This reveals a conversion gradient, as is also seen in other organisms (NICOLAS and PETES 1994; PAQUES and HABER 1999). The decrease is not strictly monotonic. Alleles *ura4A-6* and *ura4A-3* show departures. This might be attributed to statistical fluctuations or, in the case of *ura4A-6*, to the marker effect of G-to-C transversions (SCHÄR and KOHLI 1993).

Before describing the novel phenomenon called mating-type bias (mat bias), some conventions applied in this article will be introduced.

1. Allele ratios in tetrads are stated according to the mode used for eight-spored asci (each single-strand is counted in the four-spored asci).
2. Plus (+) is always stated first, followed by minus (−), and the wild-type allele + at *ura4A* promotes growth on uracil-free media.
3. Type I and type II crosses are defined as follows: In type I crosses, the h^- parent contributes the *ura4A* mutant allele, whereas in type II crosses, the wild-type allele is associated with h^-.

The mat bias is documented in Table 2 and Figure 1. The two conversion classes do not occur with equal frequencies. In type I, 6:2 conversions are less frequent (shaded frequency bars in Figure 1B) than 2:6 (open bars). In type II, the situation is reversed; 6:2 tetrads are in the majority (Figure 1C). This rule is not strict. Of the 12 markers analyzed, 8 conform to the scheme, 3 violate it, and 1 shows equality (*ura4A-2*). When all tetrad numbers were pooled within types, type I showed a total of 66 6:2 tetrads and 112 2:6 tetrads. In type II, the numbers were 55 (6:2) and 28 (2:6). The departure from equality is significant in both cases (χ^2 test, $P < 0.005$). It appears that information carried by the allele entering with the h^- parent was preferably donated for conversion, while the allele coming with the h^+ parent acted as acceptor more often than parity would predict.

Polarity, mat bias, and map expansion as revealed by random spore analysis: Random spores from a number of two-factor crosses have been analyzed. For ease of discussion, we define type III crosses as h^- *a* + × h^+ + *b*. The 5′ mutation *a* enters with the h^- parent, and the 3′ mutation *b* with the h^+ parent. The reciprocal type

TABLE 2

Conversion frequencies of *ura4A* mutations in one-point crosses

Mutation	Position[a]	Sequence change	Cross type[b]	Conversions[c] 6:2	Conversions[c] 2:6	Tetrads analyzed	Conversion (%)
13	562	C to A	II	24	13	208	17.8
1	634	A to G	I	13	24	213	17.4
5	709	G to T	I	6	20	214	12.1
6	793	G to C	I	10	7	200	8.5
14	823	C to A	I	8	16	217	11.1
9	934	G deletion	II	14	5	216	8.8
12	1001	G insertion	I	4	15	217	8.8
2	1043	G to A	I	8	8	211	7.6
4	1066	G to A	II	4	8	153	7.8
3	1104	C to T	I	15	12	220	12.3
11	1163	22-bp repeat	II	13	2	205	7.3
10	1167	C to T	I	2	10	204	5.9

[a] Numbering according to Grimm *et al.* (1988). First base of start codon is 534; first base of stop codon is 1326.

[b] Cross type I is h^- *ura4A*$^-$ × h^+ *ura4A*$^+$; cross type II is h^- *ura4A*$^+$ × h^+ *ura4A*$^-$.

[c] In this tetrad run it was not possible to detect PMS. A conversion of 6:2 means three *ura4A*$^+$ spore colonies (prototrophs) and one *ura4A*$^-$ colony (auxotroph); 2:6 conversion tetrads have only one *ura4A*$^+$ spore colony.

IV crosses were h^- + *b* × h^+ *a* +. The data are given in Table 3 [one determination per cross, prototrophs per million (ppm) spores rounded to two figures]. A series of preliminary experiments (data not shown) with a number of mutants led to the recognition that polarity, mat bias, and map expansion are detectable by this approach. Then the seven mutations, *13*, *1*, *5*, *14*, *9*, *2*, and *10* in 5′–3′ order, were chosen (low reversion frequency, suitable location) for crosses carried out under rigorously standardized conditions. The data on six mutations are shown in Figure 2. The observations of mutant *ura4A-9* are treated in the next section. All pairwise combinations have been analyzed. In control selfings of the mutants, no prototrophs were observed in ~2×10^7 spores, with exception of *ura4A-9* (2×10^{-5}). The concentrations of prototrophic recombinants and of total spores in spore suspensions were determined as described in MATERIALS AND METHODS. Prototrophs per million spores were calculated by the division of the prototroph concentration by the concentration of total spores and then multiplied by 10^6. The recombination density (*D*) is defined as the quotient of the ppm value and the number of base pairs separating the two mutations involved. *D* is a measure of hotness for recombination of a given interval.

In Figure 2 intragenic recombination is plotted in an unconventional way by jointly using genetic and physical information. The abscissa represents the physical map of *ura4A* in base pairs with the six mutations located at their sites. The recombination densities are shown as horizontal bars whose endpoints connect the mutations involved and whose heights indicate the density value.

The hot spot nature of *ura4A* is clearly revealed by the two-factor crosses: Whereas in non-hotspot genes ppm values obtained with intragenic markers farthest apart rarely exceed 1000 (Reymond *et al.* 1992; Grishchuk and Kohli 2003), the value for the extreme mutations *ura4A-13* and *ura4A-10* is >10,000 in the type IV cross.

Inspection of the data in Table 3 reveals differences between the prototroph frequencies (ppm) and the recombination densities (*D*) for the mating-type reciprocal crosses. Prototrophs are mainly produced by events starting at one end of the gene and ending between the two mutations. Like the tetrad data, the random spore data can be explained by assuming that the 5′ part of *ura4A* entering with the h^+ parent is the preferred acceptor of information. Thus, in type III crosses there is a preponderance of the proximal *a* mutation replacing + by conversion. This produces not a prototroph but rather the double mutant (*a b*). On the other hand, in type IV, + replaces *a*, generating a wild-type allele.

In Figure 2 the recombination densities are plotted for type III (dashed lines) and type IV crosses (solid lines). In both series the highest *D*-values were generally obtained for intervals bordered by alleles close to the 5′ end of the gene. The *D*-values gradually fall for intervals toward the 3′ end. Estimates for intervals of approximately equal physical length decline from left to right. The lowest values were obtained for the interval defined by the mutations *2* and *10* closest to the 3′ end. This gradient of *D*-values reflects the 5′–3′ polarity of NMS already observed in the one-factor crosses (Figure 1).

In the two-factor crosses the mat bias first described by tetrad analysis (Figure 1) reveals itself for most intervals by comparison of the *D*-value from the type III cross with that from the type IV cross. The corresponding data are given in Table 3 and plotted in Figure 2 (cross III, dashed lines; cross IV, solid lines). With four exceptions, the *D*-values from type IV crosses are higher than

TABLE 3

Random spore analysis of two-point crosses

		Type III cross (low)[c]		Type IV cross (high)[c]		
Mutations[a]	Distance[b] (bp)	ppm[d]	Density[e]	ppm[d]	Density[e]	Quotient[f]
13 × 1	72	620	8.6	880	12.3	0.70
13 × 5	147	960	6.5	2,200	14.8	0.44
13 × 14	261	2100	7.9	4,600	17.5	0.45
13 × 9	371	6900	18.5	7,900	21.2	0.87
13 × 2	481	6800	14.1	9,500	19.8	0.71
13 × 10	605	8600	14.2	12,000	20.2	0.71
1 × 5	75	540	7.1	670	9.0	0.80
1 × 14	189	1700	8.9	2,300	12.0	0.74
1 × 9	299	5500	18.3	5,100	17.1	1.07
1 × 2	409	5000	12.2	5,800	14.3	0.86
1 × 10	533	5700	10.8	9,400	17.7	0.61
5 × 14	114	950	8.3	1,100	10.1	0.83
5 × 9	224	3700	16.6	3,500	15.8	1.05
5 × 2	334	4800	14.3	4,100	12.4	1.16
5 × 10	458	6000	13.2	5,900	12.8	1.03
14 × 9	110	1100	9.9	1,400	12.8	0.78
14 × 2	220	1600	7.3	2,000	9.3	0.79
14 × 10	344	2400	6.9	4,000	11.6	0.59
9 × 2	110	930	8.4	1,100	10.2	0.83
9 × 10	234	1900	8.2	2,400	10.3	0.80
2 × 10	124	480	3.9	750	6.0	0.64

[a] The mutation stated first is the one closer to the 5′ end of the gene.
[b] The distance between the mutation sites in base pairs.
[c] In type III crosses, the mutation closer to the 5′ end is in the h^- strain; in type IV crosses, it is in the h^+ strain.
[d] Prototrophic recombinants per million spores (one experiment per cross).
[e] Prototrophs per million divided by base pairs (distance between mutations).
[f] Prototrophs per million of the type III cross divided by ppm of the type IV cross.

those from type III crosses. The quotients (Q) of types III and IV ppm values are shown in Table 3. Under the assumption that mating-type configuration has no effect on prototroph formation, one expects an equal number of Q-values below and above unity, yet the observed ratio is 17:4, clearly deviating from 1:1. The range of the 21 Q-values is 0.44–1.16, the median 0.79, and the mean 0.78 with an associated standard deviation of 0.19. In addition to polarity and mat bias, map expansion is visible (Holliday 1964). This cannot be seen in monofactorial crosses. Map expansion is the term for the observation that intragenic recombinant frequencies (ppm) for a given interval are higher than the sum of the frequencies obtained for subintervals. If map expansion were absent in *ura4A*, the density of a compound interval could not be larger than the largest value for the subintervals. Inspection of Figure 2 shows that this is never the case for the type IV crosses. In any family of intervals chosen, the compound value always surpasses the subinterval values. There are a few exceptions for the type III crosses, however, but basically the same conclusion can be reached for the series yielding low ppm values. It is evident that mixing the two data sets would confuse the situation.

A novel marker effect: The data on *ura4A-9* are given in Table 3 but not in Figure 2. The mutations included in Figure 2 behave in a regular way in the sense that in families of intervals with the same left-hand marker the densities monotonically increase as the right-hand partner allele moves toward the 3′ end. *ura4A-9*, located between *14* and *2*, is an exception. Its D-values are too large to fit into the pattern of the other mutations. This, we think, reflects a mild marker effect. Mutation *9*, a deletion of a G, enhances prototroph formation independent of polarity and map expansion effects. For this reason, it was excluded from Figure 2 and the analysis of mat bias and map expansion. For the same reason, mutation *6*, a G-to-C transversion, was also excluded. G-to-C transversion marker effects are strong and have been described in detail (Schär and Kohli 1993).

Hybrid DNA, conversion, and restoration at *ura4A*: The high conversion frequency at *ura4A* (in contrast to the forbidding quarter percentage generally seen) makes it possible to obtain some information on the nature of recombination events. Two crosses, X1119 and MX1124, have been analyzed. With respect to *ura4A*, they are identical type IV crosses: h^- *ura4A-10* × h^+ *ura4A-13*. The difference is in the genetic background. In

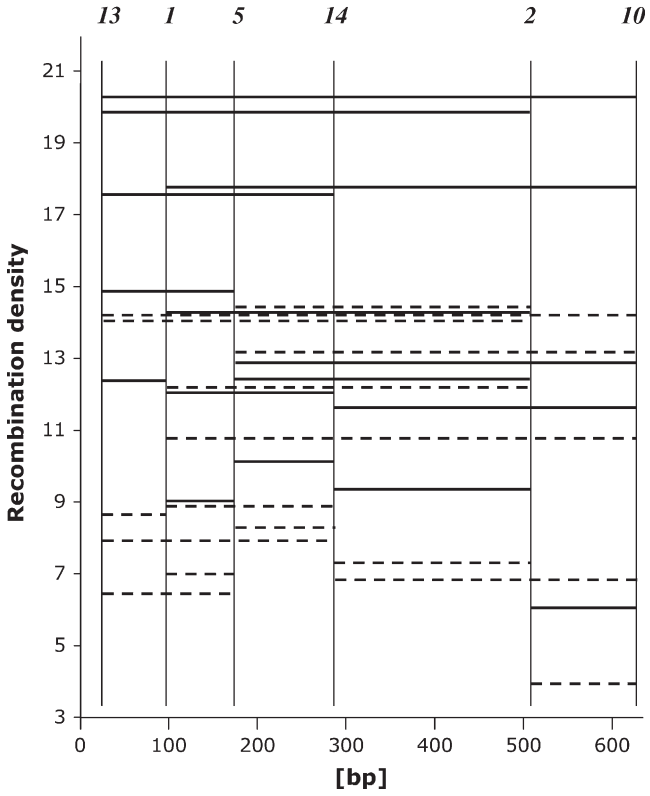

FIGURE 2.—Intragenic two-factor crosses at *ura4A*. The abscissa shows the open reading frame of *ura4A* (5′ end to the left) and the physical position of six selected mutations. The ordinate portrays the recombination density *D* (ppm per base pair). The horizontal lines connect the two mutations involved in a given cross. Type III crosses show lower densities (dashed lines) than the corresponding type IV crosses (solid lines). The detailed data are shown in Table 3. For further explanations, see the text.

X1119, the mismatch repair genes *pms1* and *swi10* (FLECK *et al.* 1999) were wild type; in MX1124, they were disrupted.

Table 4 sums up the tetrad analysis of X1119. The overall frequency of NMS is 51/290 (18%). Most events involve both sites: 35 co-conversions (tetrad types D and E) and two co-PMS (F and G), totaling 37/51 (73%). Single-site PMS was not detected. A total of 14 single-site conversions (B and C) were found at the 5′ mutation *13*. In contrast, the 3′ mutation *10* was never involved alone. The asymmetries within the single conversion and the co-conversion classes are attributed to the mat bias: The allele entering the cross with h^+ acts predominantly as acceptor.

The data are interpreted as follows: All or most hDNA starts upstream of the gene and extends to the 3′ end of the gene. It may terminate within the gene or, more frequently, beyond it. Repair of base mismatches in hDNA is efficient (35 co-conversions) but not absolute (2 co-PMS). If hDNA were exclusively symmetrical, one would expect some apparent reciprocal recombination between *13* and *10*, due to coverage of *13* alone combined with conversion-type repair in both hDNA chromatids. Since this was not found, we prefer the view that hDNA is mostly asymmetrical at *ura4A*.

The results from cross MX1124 (mismatch repair defective) are also presented in Table 4. In this case, the first postmeiotic cells deriving from the spores have been separated to yield octads composed of four pairs of colonies deriving from a single meiosis. The inactivation of mismatch repair led to a marked increase of PMS events. Yet mismatch repair apparently was not completely abolished. For instance, octad B was classified as a single-site conversion of *13* and octad D as a co-conversion.

The analysis suffered from considerable spore lethality, likely due to the repair mutant background. Disruption of *pms1* has a deleterious effect on spore viability (SCHAR *et al.* 1997). In addition to the complete octads, we tentatively incorporated information from the incomplete octads, when they were missing only one colony, or from the two sister colonies deriving from a single spore (as indicated in Table 4). The genotype of missing colonies was always assumed to be one of the parentals and chosen to avoid creation of an NMS event.

First, the complete octads are considered alone. The overall frequency of NMS is 11/43 (26%). Ten events are easily explained by asymmetrical hDNA, and one (L) shows evidence for symmetrical hDNA. Mutation *13* is involved alone four times (B and H). In the remaining seven NMS octads, both markers participate. No conversion or PMS of *10* alone was found. Thus, the same conclusions as with X1119 are reached: hDNA enters predominantly from the 5′ side, covering in a minority of cases *13* alone, and in the majority of events *13* and *10* jointly. Furthermore, hDNA is mostly asymmetrical.

Two interpretations are possible for octad L.

1. hDNA is fully symmetrical over the entire gene, and one *13*/+ mismatch experiences restoration-type repair. Thus, the repair deficiency might not only reduce the repair frequency, but also shorten the tracts in the remaining cases of repair. Single-site repair would then occur at the expense of corepair.
2. hDNA formation starts asymmetrically in one chromatid and shifts to a symmetrical phase between the markers. Absence of repair of the three resulting mismatches then results directly in octad L.

In what follows, all octads of cross MX1124 (shown in Table 4) are considered. The frequency of NMS is 32% (25/78). All but two (L and M) can be explained by asymmetrical hDNA formation. The 5′ site *13* was involved alone five times (B and H). Both sites were involved in 15 octads (D, F, G, K, L, M). The 3′ site *10* was involved alone in five octads (I). The data indicate that hDNA may cover marker *10* alone. This could occur if an event started within the gene and proceeded toward the 3′ end, and, alternatively, started in the 3′ flanking region and terminated between the markers.

TABLE 4

Tetrad analysis of two-point crosses

Tetrad types	Spore 1	Spore 2	Spore 3	Spore 4	No.[c]
	Cross X1119[a]: h^+ *ura4A-13* × h^- *ura4A-10*				
A	+ −	+ −	− +	− +	239
	+ −	+ −	− +	− +	
B	+ −	+ −	+ +	− +	10
	+ −	+ −	+ +	− +	
C	+ −	− −	− +	− +	4
	+ −	− −	− +	− +	
D	+ −	+ −	+ −	− +	25
	+ −	+ −	+ −	− +	
E	+ −	− +	− +	− +	10
	+ −	− +	− +	− +	
F	+ −	+ −	+ −	− +	1
	+ −	+ −	− +	− +	
G	+ −	+ −	− +	− +	1
	+ −	− +	− +	− +	
Total:					290
	Cross MX1124[b]: h^+ *ura4A-13 pms1*$^-$ *swi10*$^-$ × h^- *ura4A-10 pms1*$^-$ *swi10*$^-$				
A	+ −	+ −	− +	− +	32, 8, 13
	+ −	+ −	− +	− +	
B	+ −	+ −	+ +	− +	1, 1, 0
	+ −	+ −	+ +	− +	
D	+ −	+ −	+ −	− +	1, 0, 0
	+ −	+ −	+ −	− +	
F	+ −	+ −	+ −	− +	3, 0, 2
	+ −	+ −	− +	− +	
G	+ −	+ −	− +	− +	2, 1, 2
	+ −	− +	− +	− +	
H	+ −	+ −	+ +	− +	3, 0, 0
	+ −	+ −	− +	− +	
I	+ −	+ −	− +	− +	0, 2, 3
	+ −	+ +	− +	− +	
K	+ −	+ −	− +	− +	0, 0, 2
	+ −	− −	− +	− +	
L	+ −	+ −	+ −	− +	1, 0, 0
	+ −	+ +	− +	− +	
M	+ −	+ −	+ −	− +	0, 0, 1
	+ −	+ +	− −	− +	
Total:					43, 12, 23

[a] For each spore of the tetrads the genotype is given for both DNA strands (+, wild type; −, mutant), first for the 5′ site (*13*), followed by the 3′ site (*10*).

[b] Octad analysis was performed on this cross. Thus, the + and − symbols refer to homoduplex DNA derived from the first mitotic division of spores.

[c] Only complete tetrads were considered for cross X1119. For cross MX1124, the numbers of complete octads for a specific type are given first, followed by the numbers of octads with one or two missing colonies (see text).

These possibilities cannot be disproved at this stage. On the other hand, on the basis of X1119 and the sample of complete octads with no sign of NMS of *10* alone, we prefer the interpretation that the five octads under discussion are the result of hDNA spanning both sites with restoration repair limited to the *13*/+ mismatch.

In considering *13* strictly on its own, we find support for the occurrence of restoration at the 5′ end of *ura4A*. In the repair-proficient cross X1119, there are two PMS and 49 conversion events in 290 tetrads, resulting in a conversion frequency of 17% (49/290). In the repair-deficient cross MX1124, there are 17 PMS and three conversion events. We imagine that almost all of the 17 PMS events would be repaired in a repair-proficient cross. If one assumes that 16 of the 17 PMS events yielded eight conversions and eight restorations, the conversion frequency would be 14% (11/78). If, on the other hand, all 16 PMS events were repaired into conversions, the frequency would be 24% (19/78). In conclusion, the assumption that *13*/+ mismatches are about half converted and half restored in repair-proficient crosses leads to a better agreement with the 17% conversion observed at *13* in the X1119 cross.

DISCUSSION

The frequency of meiotic recombination at the *ura4A* gene is markedly elevated compared with other *S. pombe* genes analyzed. The *ura4A* hot spot originated from insertion of the *ura4* gene 15 kb away from *ade6* on chromosome III (Grimm *et al.* 1994). At its original locus *ura4* shows low recombination frequencies: the maximal prototroph frequency obtained in crosses between mutants was 1400×10^{-6} (data not shown). Not all relocations of genes lead to hot spot activity in *S. pombe*. The insertion of *arg3* on chromosome III 20 kb from *ura4A* does not result in a hot spot (B. Sakem and J. Kohli, unpublished results). Relocation of the *ade6-M26* hot spot to various places in the genome resulted in strong variation, including loss, of hot-spot activity (Virgin and Bailey 1998).

The well-characterized hot spot *ade6-M26* (Gutz 1971; Davis and Smith 2001) derives from a single base substitution in the open reading frame of *ade6*. It leads to the formation of an oligonucleotide sequence that is required for hot spot activity (Schuchert *et al.* 1991; Steiner *et al.* 2002). *ura4A* is only the second meiotic hot spot that has been characterized in detail in *S. pombe*. Its maximal frequency of NMS events (18% in wild type, 26% in mismatch-repair-deficient strains) is higher than that of the homozygous *ade6-M26* hot spot: 7.5% in wild type (Schär and Kohli 1994), and 9.5% in repair-deficient background (Fleck *et al.* 1999). Many hot spots of recombination have been characterized in *S. cerevisiae* (Lichten and Goldman 1995; Paques and Haber 1999) and also in higher eukaryotes (de Massy 2003). It remains to be elucidated to what extent the mechanisms leading to hot-spot activity are conserved in different organisms. In addition, hot spots like *ura4A* render studies of recombination mechanisms feasible, which are not possible elsewhere in the genomes.

Polarity and double-strand breaks: A conversion gradient is seen in *ura4A* ranging from 18% NMS at the 5′ end to 6% at the 3′ end (Figure 1). This polarity is also apparent in prototroph frequency analysis of two-

factor crosses (Figure 2). *ura4A* is the first *S. pombe* gene with a clearly described polarity. In *S. cerevisiae* and other fungi, this pattern is frequent and indicates initiation of recombination by DSB formation in the promoter region (Lichten and Goldman 1995; Liu *et al.* 1995; Paques and Haber 1999; Petes 2001). Recently, a meiotic DSB has been detected in the region upstream of *ura4A* (B. Sakem and J. Kohli, unpublished results). But there are exceptions to initiation in the 5′ region: In the *HIS2* gene of *S. cerevisiae* higher frequencies of conversion are observed for mutations at the 3′ end where two DSBs also have been located (Malone *et al.* 1992; Haring *et al.* 2003).

For the *ade6-M26* hot spot, DSB formation has been shown to move through the *ade6* gene in register with movement of the *M26* oligonucleotide sequence. Also, the amount of DNA breakage correlated with intragenic recombination frequency (Steiner *et al.* 2002). It has been shown that Atf1/Pcr1 transcription-factor binding to the *M26* sequence is required for *M26* hot-spot activity (Kon *et al.* 1997). Thus, the *M26* hot spot may correspond to α-type hot spots of *S. cerevisiae* that require transcription factor binding for efficient DSB formation (Petes 2001). In *S. cerevisiae*, DSB formation is also promoted by sequences refractive to nucleosome formation (β-type hot spots) and by sequences high in G + C content γ-type hot spots (Petes 2001). A large number of meiotic DSBs were visualized throughout the *S. pombe* genome by pulse-field gel electrophoresis and proposed to be involved in meiotic recombination (Cervantes *et al.* 2000; Young *et al.* 2002). Additional experiments are required for determination of the features that lead to hot spot activity at *ura4A*.

Hybrid DNA, conversion, and restoration: Hybrid DNA is a central intermediate in homologous recombination (Paques and Haber 1999). It has been shown to occur with high frequency across the *ade6-M26* hot spot sequence (Schär and Kohli 1994). This work demonstrates frequent coverage of the whole *ura4A* gene by hDNA as concluded from the observed co-conversion and PMS events found in tetrad analysis of two-factor crosses (Table 4). hDNA extends predominantly from the 5′ side and is likely to terminate to some extent in the middle of the gene, since conversion of a 5′ mutation alone was observed (Table 4). Conversion of the 3′ allele alone was not observed, indicating that extension of hDNA from the 3′ side into the gene is rare. The hDNA formation at *ura4A* mostly occurs in only one chromatid (asymmetrical), but two cases of symmetrical hDNA have been demonstrated (Table 4), one in the wild-type (3% of NMS tetrads) and the other in the repair-deficient cross (4% of NMS tetrads). The corresponding values for *ade6-M26* are: no aberrant 4:4 tetrads in wild type and 23% in the repair-deficient cross (Fleck *et al.* 1999). Lower frequency of symmetrical hDNA formation may distinguish the *ura4A* hot spot from the *M26* hot spot.

Mismatches in hDNA are repaired to different extents, depending on the types of cells and base mismatches formed. In *S. pombe*, repair is efficient for all mismatches (95% repair or more), with the notable exception of C/C mismatches with 70% repair (Schär *et al.* 1993; Schär and Kohli 1993). With the exception of the marker-effect mutations (see below), the *ura4A* mutations used in this study produced mismatches that were corrected with high efficiency. Few PMS events were found with the exception of cross MX1124, in which two different pathways of mismatch repair were inactivated (Fleck *et al.* 1999).

There are different models for the explanation of gradients of NMS events across genes. One model, the restoration/conversion model, explains such gradients assuming that 5′ markers are mostly converted, whereas mismatches at the 3′ end are half converted and half restored (Detloff *et al.* 1992; Kirkpatrick *et al.* 1998). This scenario assumes that hDNA practically always covers the entire gene. If hDNA enters from one side and is allowed to terminate within the gene, the gradient is explained. Then there is no need to assume different frequencies of conversion and restoration in function of the site within the gene.

For *ura4A* we prefer the termination-within-gene hypothesis to the restoration/conversion model. First, *ura4A-13*, the extreme 5′ mutation, is apparently not only converted, but also restored (see the corresponding section in results). Second, frequencies of prototrophic recombinants in segments of equal physical size drop from the 5′ to the 3′ region of the gene (Figure 2). This is explained by more frequent termination of hDNA between mutations at the 5′ end than at the 3′ end. In the restoration/conversion model, hDNA is assumed to span the whole gene, and recombinants must arise by independent repair of the two mismatches. Depending on the chromatid involved, one mismatch must experience conversion-type repair, the other restoration-type repair. If chromatids of different parentage are equally used, and no bias in repair direction exists, no drop of recombination is expected. If 5′ markers are preferentially converted, again no drop of recombination is expected, since gain in one chromatid is balanced by loss in the other. Finally, the mat bias to be described below has no impact on this matter: crosses of both types, III (low) and IV (high), show the same polar decrease of recombination density.

Marker effects: The *ura4A-6* mutation is a G-to-C transversion (Table 2, Figure 1). It shows an overall frequency of NMS in one-factor crosses expected from its location within the gene, but strongly enhanced prototroph frequencies in two-factor crosses with other *ura4A* mutants (data not shown). This feature of G-to-C transversions has been investigated (Schär *et al.* 1993; Schär and Kohli 1993; Fleck *et al.* 1999). It is based on the inability of the MutLS long-patch mismatch-repair system to correct C/C mismatches. Instead, C/Cs are partially repaired by the short-patch nucleotide excision repair system and remain partially unrepaired, resulting

in PMS. Both the short repair tracts and the failure of repair contribute to higher prototroph frequencies, when two mutations involved in a two-factor cross are included in the same hDNA tract.

The mutation *ura4A-9*, deletion of a single G-C pair, showed normal behavior in one-factor crosses (Table 2, Figure 1). In the two-factor crosses, it yielded generally higher prototroph frequencies than expected from its position in the middle of the gene. The average recombination density calculated from the six crosses shown in Table 3 is 14.5, while the averages for the flanking mutations *ura4A-14* and *ura4A-2* are 12.2 and 12, respectively. This novel marker effect is comparably weak. It may originate from inefficient repair of the single nucleotide loops (G and C) in hDNA by the MutLS system (PMS as consequence) or by recognition of the single base loops by an alternative, short-patch repair system.

The two examples of marker-effect alleles demonstrate that prototroph frequencies, as determined in two-factor crosses, can be affected by special features of the different mismatch repair pathways. For this reason mutations showing marker effects must be excluded when overall features of intragenic recombination are studied (Figure 2). The phenomena of mat bias and map expansion discussed below could not be clearly described with inclusion of the data from the two marker-effect alleles.

Mat bias: This phenomenon, to our knowledge, has not been described before. The *ura4A* allele entering the cross with the h^+ parent acts as information acceptor almost twice as often as the allele being contributed by the h^- parent (167: 94, $Q = 0.56$), as seen by summing up of the tetrad analysis of all mutants (Table 2). In the random spore analysis of two-factor crosses (Table 3), the mean bias ($Q = 0.78$) is lower. This may derive from the lack of detection of events that do not result in prototrophic recombinants (co-conversions, Table 4). Since the h^+ and h^- mating types of *S. pombe* carry different DNA rearrangements at the mating-type locus on chromosome II (Beach *et al.* 1982), we wondered whether the structural differences between the h^{+N} and h^{-S} mating types used in our experiments could account for the mat bias. From the h^{+N} *ura4A-13* and h^{+N} *ura4A-10* strains spontaneous h^{-U} derivatives were isolated (Egel 1989), and random spores of the two reciprocal crosses *13* × *10* with isogenic backgrounds were analyzed (data not shown). The asymmetry in prototroph frequencies persisted, again with the chromosome from the h^+ parent as the preferred acceptor. Since h^{+N} and h^{-U} are structurally equivalent, it seems that mating-type function, rather than mating-type structure, is responsible for the mat bias. h^+ mating-type function derives from the expression of the two genes P_c and P_i from the mat1P allele at mat1 (Kelly *et al.* 1988). That the mat bias is caused by a genetic factor unrelated to mating type and residing elsewhere in the genome is unlikely, when all the reported experiments are considered.

A number of questions about the mat bias require additional experiments. Is it specific for the *ura4A* hot spot, or does it affect other genes as well? Recent experiments with two other genes indicate that the mat bias is a general phenomenon in *S. pombe* (E. Parvanov and J. Kohli, unpublished results). Obviously the chromosomes contributed by the h^+ parent maintain a memory, probably a feature of chromatin structure not present in chromosomes of h^- cells, through cell mating, karyogamy, and premeiotic DNA replication. An obvious question is whether the mat bias is absent in azygotic meiosis after homologous chromosomes have coexisted in diploid cells for many mitotic divisions. Recent experiments indicate loss of the mat bias in azygotic meiosis (E. Parvanov and J. Kohli, unpublished results).

Map expansion: This phenomenon was described on the basis of fine-structure mapping of genes (Holliday 1964). The maps were constructed from prototroph frequencies measured in two-factor crosses of auxotrophic mutants. The prototroph frequency measured for an interval defined by mutations *a* and *b* was often larger than the sum of the prototroph frequencies obtained from two subintervals. The subintervals were defined by additional mutations mapped between *a* and *b*. The longer the *a-b* intervals were, the more pronounced was map expansion. Models for the explanation of map expansion are founded on variations of parameters of hDNA formation, of mismatch repair, and of mismatch-induced rejection of hDNA (Fincham and Holliday 1970; Fujitani and Kobayashi 1997). The extreme map expansion found in *S. pombe* tRNA genes (Fincham and Holliday 1970) was later attributed to marker effects of G-to-C transversion mutations (Hofer *et al.* 1979; Schär and Kohli 1993). Since physical ordering of mutations was not possible at the time, the description of map expansion was hampered by mistakes in mapping and by marker-effect mutations that could not be identified easily. Considering these difficulties, the very existence of map expansion was questioned (Stahl 1979).

The distribution of physically mapped mutations along *ura4A*, the exclusion of marker-effect alleles, the frequent coverage of the whole gene by hDNA, and the frequent long repair tracts covering the 605 bp between the outer markers *13* and *10* (co-conversion) were ideal for a reevaluation of the existence of map expansion. As shown in Figure 2 and explained in the results, map expansion was clearly demonstrated in *ura4A*. On the basis of the results obtained from tetrad and octad analysis of the two-factor cross 13 × 10 (Table 4), we offer the following explanation. Prototrophic recombinants appear to be generated mainly by hDNA ending between the mutation sites in *ura4A*. A minor contribution is likely to derive from hDNA covering both sites, coupled with independent repair of the two mismatches. Map expansion could then be the result of this second component gaining overproportionally in importance as markers become farther apart. Alternatively, hDNA spanning two markers may be destabilized

more frequently, when the markers are close, resulting in a relatively greater loss of potential recombinants for close markers.

In conclusion, the detailed analysis of intragenic recombination at *ura4A* has revealed the novel phenomenon of mat bias and established the existence of map expansion and will serve as the basis for the investigation of the molecular mechanisms of recombination.

We acknowledge support from grants of the Swiss National Science Foundation. K. Ludin was supported by a Marie-Heim-Vögtlin fellowship. Part of this work is contained in the Ph.D. thesis of M. Baur, submitted to the Faculty of Science, University of Berne.

LITERATURE CITED

Beach, D., P. Nurse and R. Egel, 1982 Molecular rearrangement of mating-type genes in fission yeast. Nature **296:** 682–683.

Cervantes, M. D., J. A. Farah and G. R. Smith, 2000 Meiotic DNA breaks associated with recombination in S. pombe. Mol. Cell **5:** 883–888.

Davis, L., and G. R. Smith, 2001 Meiotic recombination and chromosome segregation in Schizosaccharomyces pombe. Proc. Natl. Acad. Sci. USA **98:** 8395–8402.

de Massy, B., 2003 Distribution of meiotic recombination sites. Trends Genet. **19:** 514–522.

de Massy, B., V. Rocco and A. Nicolas, 1995 The nucleotide mapping of DNA double-strand breaks at the *CYS3* initiation site of meiotic recombination in *Saccharomyces cerevisiae*. EMBO J. **14:** 4589–4598.

Detloff, P., M. A. White and T. D. Petes, 1992 Analysis of a gene conversion gradient at the *HIS4* locus in *Saccharomyces cerevisiae*. Genetics **132:** 113–123.

Egel, R., 1989 Mating-type genes, meiosis and sporulation, pp. 31–73 in *Molecular Biology of the Fission Yeast*, edited by P. Y. A. Nasim and B. F. Johnson. Academic Press, San Diego.

Fincham, J. R., and R. Holliday, 1970 An explanation of fine structure map expansion in terms of excision repair. Mol. Gen. Genet. **109:** 309–322.

Fleck, O., E. Lehmann, P. Schar and J. Kohli, 1999 Involvement of nucleotide-excision repair in msh2 pms1-independent mismatch repair. Nat. Genet. **21:** 314–317.

Fujitani, Y., and I. Kobayashi, 1997 Mismatch-stimulated destruction of intermediates as an explanation for map expansion in genetic recombination. J. Theor. Biol. **189:** 443–447.

Grimm, C., J. Kohli, J. Murray and K. Maundrell, 1988 Genetic engineering of Schizosaccharomyces pombe: a system for gene disruption and replacement using the ura4 gene as a selectable marker. Mol. Gen. Genet. **215:** 81–86.

Grimm, C., J. Bahler and J. Kohli, 1994 M26 recombinational hotspot and physical conversion tract analysis in the *ade6* gene of *Schizosaccharomyces pombe*. Genetics **136:** 41–51.

Grishchuk, A. L., and J. Kohli, 2003 Five RecA-like proteins of *Schizosaccharomyces pombe* are involved in meiotic recombination. Genetics **165:** 1031–1043.

Gutz, H., 1971 Site specific induction of gene conversion in *Schizosaccharomyces pombe*. Genetics **69:** 317–337.

Gutz, H., H. Heslot, U. Leupold and N. Loprieno, 1974 *Schizosaccharomyces pombe*, pp. 395–446 in *Handbook of Genetics*, edited by R. C. King. Plenum Press, New York.

Haring, S. J., G. R. Halley, A. J. Jones and R. E. Malone, 2003 Properties of natural double-strand-break sites at a recombination hotspot in *Saccharomyces cerevisiae*. Genetics **165:** 101–114.

Hofer, F., H. Hollenstein, F. Janner, M. Minet, P. Thuriaux *et al.*, 1979 The genetic fine structure of nonsense suppressors in *Schizosaccharomyces pombe*. Curr. Genet. **1:** 45–61.

Holliday, R., 1964 A mechanism for gene conversion in fungi. Genet. Res. **5:** 282–304.

Kelly, M., J. Burke, M. Smith, A. Klar and D. Beach, 1988 Four mating-type genes control sexual differentiation in the fission yeast. EMBO J. **7:** 1537–1547.

Kirkpatrick, D. T., M. Dominska and T. D. Petes, 1998 Conversion-type and restoration-type repair of DNA mismatches formed during meiotic recombination in *Saccharomyces cerevisiae*. Genetics **149:** 1693–1705.

Kon, N., M. D. Krawchuk, B. G. Warren, G. R. Smith and W. P. Wahls, 1997 Transcription factor Mts1/Mts2 (Atf1/Pcr1, Gad7/Pcr1) activates the M26 meiotic recombination hotspot in *Schizosaccharomyces pombe*. Proc. Natl. Acad. Sci. USA **94:** 13765–13770.

Lichten, M., and A. S. Goldman, 1995 Meiotic recombination hotspots. Annu. Rev. Genet. **29:** 423–444.

Liu, J., T. C. Wu and M. Lichten, 1995 The localization and structure of double-strand breaks induced during yeast meiosis: evidence for a covalently linked DNA-protein intermediate. EMBO J. **14:** 4599–4608.

Malone, R. E., S. Bullard, S. Lundquist, S. Kim and T. Tarkowski, 1992 A meiotic gene conversion gradient opposite to the direction of transcription. Nature **359:** 154–155.

Nicolas, A., and T. D. Petes, 1994 Polarity of meiotic gene conversion in fungi: contrasting views. Experientia **50:** 242–252.

Ohta, K., T. Shibata and A. Nicolas, 1994 Changes in chromatin structure at recombination initiation sites during yeast meiosis. EMBO J. **13:** 5754–5763.

Paques, F., and J. E. Haber, 1999 Multiple pathways of recombination induced by double-strand breaks in Saccharomyces cerevisiae. Microbiol. Mol. Biol. Rev. **63:** 349–404.

Petes, T. D., 2001 Meiotic recombination hot spots and cold spots. Nat. Rev. Genet. **2:** 360–369.

Reymond, A., S. Schmidt and V. Simanis, 1992 Mutations in the cdc10 start gene of Schizosaccharomyces pombe implicate the region of homology between cdc10 and SWI6 as important for p85cdc10 function. Mol. Gen. Genet. **234:** 449–456.

Schär, P., and J. Kohli, 1993 Marker effects of G to C transversions on intragenic recombination and mismatch repair in *Schizosaccharomyces pombe*. Genetics **133:** 825–835.

Schär, P., and J. Kohli, 1994 Preferential strand transfer and hybrid DNA formation at the recombination hotspot *ade6–M26* of *Schizosaccharomyces pombe*. EMBO J. **13:** 5212–5219.

Schär, P., P. Munz and J. Kohli, 1993 Meiotic mismatch repair quantified on the basis of segregation patterns in *Schizosaccharomyces pombe*. Genetics **133:** 815–824.

Schar, P., M. Baur, C. Schneider and J. Kohli, 1997 Mismatch repair in *Schizosaccharomyces pombe* requires the mutL homologous gene *pms1*: molecular cloning and functional analysis. Genetics **146:** 1275–1286.

Schuchert, P., M. Langsford, E. Kaeslin and J. Kohli, 1991 A specific DNA sequence is required for high frequency of recombination in the *ade6* gene of fission yeast. EMBO J. **10:** 2157–2163.

Smith, G. R., 2001 Homologous recombination near and far from DNA breaks: alternative roles and contrasting views. Annu. Rev. Genet. **35:** 243–274.

Stahl, F. W., 1979 *Genetic Recombination: Thinking About It in Phage and Fungi*. W. H. Freeman, San Francisco.

Steiner, W. W., R. W. Schreckhise and G. R. Smith, 2002 Meiotic DNA breaks at the S. pombe recombination hot spot M26. Mol. Cell **9:** 847–855.

Virgin, J. B., and J. P. Bailey, 1998 The M26 hotspot of *Schizosaccharomyces pombe* stimulates meiotic ectopic recombination and chromosomal rearrangements. Genetics **149:** 1191–1204.

Wright, A. P. H., K. Maundrell and S. Shall, 1986 Transformation of *Schizosaccharomyces pombe* by non-homologous unstable integration of plasmids in the genome. Curr. Genet. **10:** 503–508.

Wu, T. C., and M. Lichten, 1994 Meiosis-induced double-strand break sites determined by yeast chromatin structure. Science **263:** 515–518.

Young, J. A., R. W. Schreckhise, W. W. Steiner and G. R. Smith, 2002 Meiotic recombination remote from prominent DNA break sites in S. pombe. Mol. Cell **9:** 253–263.

Zahn-Zabal, M., E. Lehmann and J. Kohli, 1995 Hot spots of recombination in fission yeast: inactivation of the *M26* hot spot by deletion of the *ade6* promoter and the novel hotspot *ura4-aim*. Genetics **140:** 469–478.

Communicating editor: P. Russell